LASER-PLASMA-ACCELERATOR-BASED $\gamma\gamma$ COLLIDERS*

C. B. Schroeder†, E. Esarey, Cs. Tóth, C. G. R. Geddes, W. P. Leemans
LBNL, Berkeley, CA 94720, USA

Abstract

Design considerations for a next-generation linear collider based on laser-plasma-accelerators are discussed, and a laser-plasma-accelerator gamma-gamma ($\gamma\gamma$) collider is considered. An example of the parameters for a 0.5 TeV laser-plasma-accelerator $\gamma\gamma$ collider is presented.

INTRODUCTION

Advanced acceleration techniques are actively being pursued to expand the energy frontier of future colliders. Although the exact minimum energy of interest for the next lepton collider will be determined by the Large Hadron Collider experiments that are presently underway, it is anticipated that center-of-mass energies approaching 1 TeV will be required. This energy is already near the limit of what can be constructed using conventional accelerator technology, given space and cost restrictions [1].

Laser-plasma accelerators (LPA) [2] have demonstrated accelerating gradients on the order of 100 GV/m, some three orders of magnitude larger than conventional accelerators. Recent LPA experiments have demonstrated high-quality GeV electron beams at Lawrence Berkeley National Laboratory (LBNL) [3, 4]. LPA technology has the potential to significantly reduce the main linac length (and, therefore, the cost) of a future lepton collider. It is natural to consider a gamma-gamma ($\gamma\gamma$) collider since the same laser technology that drives the plasma wave to accelerate the electron beam may be used for Compton back-scatter, generating the gamma rays for collision.

LASER-PLASMA ACCELERATORS

The amplitude of the accelerating field of a plasma wave driven by a resonant laser (pulse duration on the order of the plasma period) is approximately $E_z \approx [(\gamma_\perp^2 - 1)/\gamma_\perp]E_0$. Here $\gamma_\perp = (1 + a^2/2)^{1/2}$ is the Lorentz factor associated with the quiver motion of the electrons in the linearly-polarized laser field, $a^2 = 7.3 \times 10^{-19}(\lambda[\mu\text{m}])^2 I_0[\text{W/cm}^2]$ the normalized laser intensity, and $E_0 = mc\omega_p/e \simeq (96\ \text{V/m})(n[\text{cm}^{-3}])^{1/2}$ is the characteristic plasma wave accelerating field amplitude, with $\omega_p = k_p c = (4\pi ne^2/m)^{1/2}$ the plasma frequency and n the plasma number density. For additional control, the laser-plasma accelerator will operate in the quasi-linear regime ($a \sim 1$). The quasi-linear regime is accessible for parameters such that $a^2/\gamma_\perp < k_p^2 r_L^2$, where r_L is the characteristic scale length of the transverse laser intensity. The transverse focusing force in the quasi-linear regime scales as $F_\perp \propto k_p^{-1}\nabla_\perp a^2$ and therefore by shaping the transverse profile of the laser, the transverse forces in the accelerator can be controlled. Control over the focusing forces enables control of the beam dynamics (e.g., the beam matching condition). This control is not available in the highly-nonlinear blow-out regime, where the transverse forces are determined solely by the plasma density.

In general, the energy gain in a single laser-plasma accelerator stage may be limited by laser diffraction effects, dephasing of the electrons with respect to the accelerating field, and laser energy depletion into the plasma wave. Laser diffraction effects can be mitigated by use of a plasma channel (transverse plasma density tailoring), guiding the laser over many Rayleigh ranges [5]. Dephasing can be mitigated by plasma density tapering (longitudinal density tailoring), which can maintain the position of the electron beam at a given phase of the plasma wave [6]. Hence the single-stage energy gain is ultimately determined by laser energy depletion [7]. The energy depletion length scales as $L_d \propto n^{-3/2}$, and, with $E_0 \propto n^{1/2}$, the energy gain in a single stage scales as $W_{\text{stage}} \propto n^{-1}$.

After a single laser-plasma accelerating stage, the laser energy is depleted and a fresh laser pulse must be coupled into the plasma for further acceleration. This coupling distance is critical to determining the overall accelerator length (average gradient of the main linac) and the optimal plasma density at which to operate. One advantage of laser drivers for plasma acceleration is the potential for a short coupling distance between stages, and, therefore, the possibility of a high average accelerating gradient and a relatively short main linac length. The overall linac length will be given by $L_{\text{total}} = [L_{\text{stage}} + L_c]E_b/W_{\text{stage}}$, where L_c is the required coupling distance for a new drive laser (and space for any required beam transport and diagnostics), E_b is the beam energy before collision, and $L_{\text{stage}} \approx L_d$ is the single-stage plasma length. Figure 1 plots the main linac length versus plasma density for several coupling distances, with $E_b = 0.5$ TeV and $a_0 = 1.5$. Here the single-stage length and energy gain was calculated using a fluid code [8] to model the laser-plasma interaction. Plasma mirrors show great promise as optics to direct high-intensity laser pulses, potentially requiring only tens of cm to couple a drive laser into a plasma accelerator stage [9].

COLLIDER DESIGN CONSIDERATIONS

The rate of events in a collider is determined by the product of the collision cross section and luminosity. The geometric luminosity is $\mathcal{L} = fN^2/(4\pi\sigma_x\sigma_y) =$

* Work supported by the Office of High Energy Physics of the U.S. Dept. of Energy under Contract No. DE-AC02-05CH11231.

† cbschroeder@lbl.gov

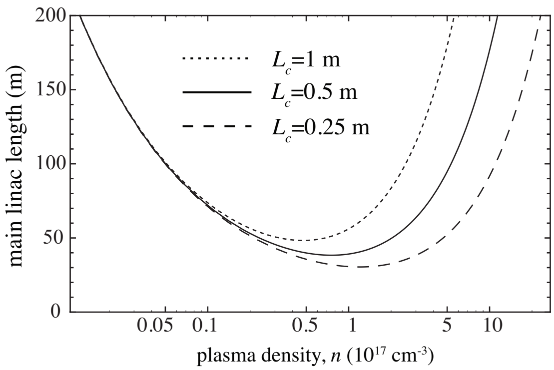

Figure 1: Main single-linac length versus plasma density n for several laser in-coupling distances L_c, for $E_b = 0.25$ TeV and $a_0 = 1.5$.

$(P_b/4\pi E_b)(N/\sigma_x\sigma_y)$, where f is the collision frequency, N is the number of particles per bunch (we assume equal number of particles per bunch), σ_x and σ_y are the horizontal and vertical rms beam sizes, respectively, at the interaction point (IP), $E_{\rm cm} = 2\gamma mc^2 = 2E_b$ is the center of mass energy, and $P_b = fNE_b$ is power in one beam. Since the cross section for collisions scales as the inverse of the square of the center-of-mass energy, $\propto E_{\rm cm}^{-2}$, the luminosity must increase proportionally to maintain the collision rate. The luminosity requirement is approximately $\mathcal{L}[10^{34}\text{cm}^{-2}\text{s}^{-1}] \approx E_{\rm cm}^2[\text{TeV}]$. As the luminosity scaling indicates, for fixed beam power, the transverse beam density at the IP must be increased as the center-of-mass energy increases. Below we will consider the option of a gamma-gamma collider, where the photon beam luminosity will be reduced from the above geometric luminosity due to the conversion efficiency of electrons to gamma rays.

There are several limitations to the achievable beam density at the IP. These include, for example, the achievable beam emittance (given limitations on initial emittance and cooling methods), radiation effects during the final focus to the IP, emittance growth in main linacs, and beam-beam interactions at the collision. In Ref. [10] the emittance growth due to the beam-plasma interaction (via Coulombic scattering of the beam electrons with the background plasma ions) was examined. It was shown that the growth is only weakly-dependent on plasma density and that, assuming a Hydrogen plasma with a temperature of $T = 10$ eV and a resonant laser pulse with $a_0 = 1.5$ and $r_L = 63$ μm, a beam injected off-crest would have an emittance growth of $\Delta\epsilon_n \approx 0.3$ nm-rad after acceleration to 0.25 TeV.

$\gamma\gamma$ Collider Considerations

There are several advantages to considering a gamma-gamma ($\gamma\gamma$) collider (or gamma-electron beam collisions), compared to an e^+e^- collider [11]. $\gamma\gamma$ collisions can access many of the lepton interactions available in an e^+e^- collider and there are additional particle physics opportunities [12]. In addition, from a collider design viewpoint, a $\gamma\gamma$ collider eliminates the need for a positron beam, and beamstrahlung and beam-beam instabilities are absent.

Photon beams can be generated from the electron beams before the IP via Compton scattering. Here we will consider near backscatter (with small collision angle $\theta \ll 1$) of the electron beam with a circularly polarized laser (polarization of the counterpropagating laser opposite that of the electrons). Solving the energy-momentum conservation equations for the electron (u_μ), laser ($k_{L\mu}$), and scattered light (k_μ), $mcu_\mu + \hbar k_{L\mu} = mcu'_\mu + \hbar k_\mu$, yields the maximum photon energy $\hbar\omega = E_b x/(1 + x + a_L^2)$, where a_L^2 is the normalized laser intensity and $x = (4E_b\hbar\omega_L/m^2c^4)\cos^2(\theta/2)$. Maximizing scattered photon energy requires maximizing x.

Photons may be lost due to the creation of e^+e^- pairs (with the associated background issues for the detector). To avoid e^+e^- pair creation requires $(\hbar k_\mu + \hbar k_{\mu L})^2 = 4\hbar^2 k_L k \le (2m_e c)^2(1+a_L^2)$, or $x \le 2(1+a_L^2)(1+\sqrt{2}) \simeq 4.83(1 + a_L^2)$. For $x = 4.8$, $\hbar\omega \simeq 0.83E_b$ assuming $a_L \ll 1$, and $\hbar\omega_L E_b = (m_e c^2)^2 x/4 \simeq 0.3(\text{MeV})^2$, or $\lambda_L[\mu\text{m}] \approx 4\ E_b[\text{TeV}]$. For example, using a solid-state laser $\hbar\omega_L = 1.2$ eV, and scattering off an electron beam with $E_e = 250$ GeV, yields $\hbar\omega = 200$ GeV.

The luminosity of the photon beams is given by $\mathcal{L}_{\gamma\gamma} = (N_\gamma/N_e)^2\mathcal{L}_{e^+e^-}$, where N_γ is the number of gammas/pulse. Comparable luminosity requires $N_\gamma \sim N_e$. The cross-section for single-photon Compton scattering ($x > 1$) is approximately $\sigma_{\rm C} \approx 2 \times 10^{-25}$ cm^2 for $x = 4.8$. In the following we will assume $2Z_R \approx l_L > l_b$ for efficient scattering in the linear regime, with Z_R the Rayleigh range, l_L the laser pulse length, and l_b the electron beam length. To produce $N_\gamma \sim N_e$ requires $\sigma_{\rm C} N_L/A_L \sim 1$, i.e., the thickness of the laser "target" is equal to one Compton scattering length. Here N_L is the number of laser photons/pulse and $A_L \sim \lambda_L Z_R/2$. Setting $\sigma_{\rm C} N_L/A_L = 1$, yields the required laser energy $U_L = N_L\hbar\omega_L = \pi\hbar c Z_R/\sigma_{\rm C}$ or $U_L[\text{J}] \approx 4Z_R[\text{mm}] \simeq 2l_L[\text{mm}]$. With this laser energy (i.e., one Compton scattering length), the conversion efficiency is $N_\gamma/N_e \approx 1 - e^{-1} \approx 0.65$. Using $U_L = \pi\hbar c Z_R/\sigma_{\rm C}$, the normalized intensity can be expressed as $a_L^2 l_L = (2r_e^2/\alpha\sigma_{\rm C})\lambda_L$ or $a_L^2 l_L[\text{mm}] \approx 0.4\ E_b[\text{TeV}]$. The laser energy required is therefore $U_L[\text{J}] \approx (0.8/a_L^2)E_b[\text{TeV}]$. The pulse duration must be long enough such that the intensity is sufficiently low to avoid nonlinear (multi-photon) scattering: $a_L^2 < 1$.

In addition the peak electric field of the laser in the rest frame of the beam must be less than the Schwinger critical field to minimize beamstrahlung. This condition can be expressed as $a_L < \lambda_L/(2\gamma\lambda_{\rm C}) = 2/x \simeq 0.4$. Setting $a_L^2 = 0.1$ yields $l_L[\text{mm}] \approx 4\ E_b[\text{TeV}]$, and $U_L[\text{J}] \approx 8\ E_b[\text{TeV}]$.

For example, a beam with $E_b = 250$ GeV ($E_{\rm cm} = 0.5$ TeV) requires a 1 μm wavelength, 2 J, 3 ps laser, with $Z_R = 0.5$ mm and $I = 2.7 \times 10^{17}$ W/cm^2. The gamma-ray energy peaks at $0.8E_b = 200$ GeV, with luminosity $\mathcal{L}_{\gamma\gamma}/\mathcal{L}_{e^+e^-} \approx (N_\gamma/N_e)^2 \approx 0.43$. Note that, although the interaction of the laser with the electron beam is at a point where the electron beam cross-section is approximately that of the laser, the scattered light is along the direction of the electron beam (since $E_b \gg \hbar\omega_L$) and will converge at the IP. The interaction must be done sufficiently close to the IP such that the natural spreading of the gamma rays, with divergence $(1 + x + a_L^2)^{1/2} mc^2/E_b$, does not significantly reduce the collisions.

Plasma Density Scalings

The accelerating gradient scales with plasma density as $E_z \propto n^{1/2}$ and the single-stage length scales as $L_{\rm stage} \propto n^{-3/2}$, yielding a single stage energy gain that scales as $W_{\rm stage} \propto n^{-1}$. In general, for efficient coupling, the bunch number will scale with plasma density as $N \propto n^{-1/2}$. Therefore, for constant luminosity, and all other beam parameters fixed, the repetition rate scales as $f \propto n$, and the beam power will scale as $P_b = fNE_b \propto n^{1/2}$. The number of stages scales as $N_{\rm stage} = E_b/W_{\rm stage} \propto n$, so the average laser power per stage scales as $P_{\rm laser} \propto n^{-1/2}$ and the total wall plug power for the acceleration scales as $P_{\rm wall} \propto n^{1/2}$. Operational cost of future linear colliders limit the wall plug power to on the order of hundred MW.

Table 1 shows a 0.5 TeV $\gamma\gamma$ collider example using $n = 10^{17}$ cm^{-3}. Typical conversion efficiencies are ∼50% for laser to plasma wave and ∼30% for plasma wave to beam (shaped electron beams are assumed to avoid energy spread growth), such that the overall efficiency from laser to beam is ∼15%. If we assume a wall-plug to laser efficiency of ∼33%, then the efficiency from wall plug to beam is ∼5%.

Table 1: Laser-plasma linear $\gamma\gamma$ collider parameters.

Plasma number density, n (cm^{-3})	10^{17}
Energy, center of mass, $E_{\rm cm}$(TeV)	0.5
Beam energy, γmc^2 (TeV)	0.25
Number per bunch, N ($\times 10^9$)	3
Collision rate, f (kHz)	15
Beam Power, $P_b = fN\gamma mc^2$ (MW)	1.8
Geometric luminosity, $\mathcal{L}$ (s^{-1} cm^{-2})	10^{34}
Bunch length, σ_z (μm)	1
Horizontal emittance, ϵ_{nx} (mm-mrad)	0.1
Vertical emittance, ϵ_{ny} (mm-mrad)	0.1
Plasma wavelength, λ_p (μm)	105
Energy gain per stage, $W_{\rm stage}$ (GeV)	7.4
Single stage length (cm)	65
Drive laser coupling distance (m)	0.5
Laser energy per stage (J)	23
Laser wavelength (μm)	1
Initial normalized laser intensity, a_0	1.5
Average laser power per stage (kW)	345
Number of stages	34
Main linac length (km)	0.039
Efficiency (wall-plug to beam)	5%
Total accelerator wall-plug power (MW)	72
Compton scattering laser wavelength (μm)	1
Compton scattering laser energy (J)	2
Compton scattering laser duration (ps)	3
Compton scattering laser Rayleigh range (mm)	0.5
Compton scattering intensity ($\times 10^{18}$ W/cm^{-2})	0.27
Gamma beam peak energy (TeV)	0.2
Conversion efficiency ($e \rightarrow \gamma$)	0.65

CONCLUSIONS

In this paper we have discussed several design considerations for future linear colliders based on LPAs. An example of collider parameters for 0.5 TeV center-of-mass energy using plasma density of $n = 10^{17}$ cm^{-3} is summarized in Table 1. We have considered a gamma-gamma collider via Compton scattering of LPA electron beams. A gamma-gamma collider would eliminate the need for positron creation and accompanying damping rings. The scattering laser energy requirements for the 0.5 TeV gamma-gamma collider are near those required for driving the LPA (e.g., 1 μm wavelength with ∼ 10 J of laser energy at the accelerator repetition rate). Significant laser technology advances are required to realize the next-generation linear collider. Although ∼10 J, short pulse lasers are currently available, repetition rates of ∼10 kHz and efficiencies of ∼30% are presently beyond state-of-the-art laser technology. Diode-pump solid state lasers show promise to generate hundreds of kW with high efficiency in the next decade. In addition there is significant LPA R&D required before realization of a LPA-based linear collider is possible. In particular, these include demonstration of accelerator stage coupling, detailed control of beam injection, and maintaining high beam quality over the length of the accelerator. The next-generation linear collider is extremely challenging for any technology, but laser-plasma-based accelerators continue to show great promise as a solution to address the size of future linear colliders.

REFERENCES

[1] G. Dugan, in *Advanced Accelerator Concepts*, edited by V. Yakimenko, AIP vol. 737, p. 29–60 (2004).

[2] E. Esarey, et al., Rev. Mod. Phys. (2009), in press.

[3] W. P. Leemans, et al., Nature Phys. 2 (2006) 696.

[4] K. Nakamura, et al., Phys. Plasmas 14 (2007) 056708.

[5] C. G. R. Geddes, et al., Phys. Rev. Lett. 95 (2005) 145002.

[6] P. Sprangle et al., Phys. Rev. E 63 (2001) 056405.

[7] B. A. Shadwick, et al., Phys. Plasmas (2009).

[8] B. A. Shadwick et al., IEEE Trans. Plasma Sci. 30 (2002) 38.

[9] D. Panasenko et al., *Advanced Accelerator Concepts*, edited by C. B. Schroeder et al, AIP vol. 1086, p. 215–220 (2009).

[10] C. B. Schroeder et al., *Advanced Accelerator Concepts*, edited by C. B. Schroeder et al., AIP vol. 1086, p. 208 (2009).

[11] V. I. Telnov, Nucl. Instrum. Methods A 294 (1990) 72.

[12] B. Badelek et al., Int. J. Mod. Phys. A 30 (2004) 5097.